Chapter 77
Design and Experimental Validation of Thick Airfoils for Large Wind Turbines

Iva Hrgovan, Wen Zhong Shen, Wei Jun Zhu, Jesper Madsen and Rolf Hansen

Abstract In this chapter, two new airfoils with thickness to chord ratios of 30 and 36 % are presented, which were designed with an objective of good aerodynamic and structural features. Airfoil design is based on a direct method using shape perturbation function. The optimization algorithm is coupled with the viscous/inviscid flow solver XFOIL.

Wind tunnel tests for both airfoils were performed in the LM Wind Power low speed wind tunnel at Reynolds numbers of 1.5–6 million and various surface conditions. The results from the experiment confirm that the optimization algorithm is suited for airfoil design and the designed airfoils have top performance.

Keywords Wind turbine · Airfoil · Blade surface · Roughness · Wind tunnel

77.1 Introduction

The growing demand for power requires larger wind turbines. The latest installed turbine prototype has an 80 m long blade that weighs around 35 t [1]. These sizes present a challenge for the structural integrity of the blade. To deal with the increased weight, designers are using thick airfoils on larger parts of the blade, such as the inboard and the middle sections.

There are several airfoil families specially designed for modern wind turbines [2, 3]. However, thick airfoils from these series are designed to be used only at the inboard section of the blade where the structural performance is more important than the aerodynamic performance. Since the aerodynamic performance of thick airfoils is becoming important, the airfoils need to be improved to provide more power and to satisfy growing structural demands. Moreover, turbines operate in

I. Hrgovan (✉) · W. Z. Shen · W. J. Zhu
Department of Wind Energy, Technical University of Denmark, Kongens Lyngby, Denmark
e-mail: ivah@dtu.dk

J. Madsen · R. Hansen
LM Wind Power, Kolding, Denmark

A. Sayigh (ed.), *Renewable Energy in the Service of Mankind Vol I*,
DOI 10.1007/978-3-319-17777-9_77

environments filled with particles that either damage the blade surface or accumulate on the surface and change the flow conditions. This degradation causes a significant drop in annual energy production [4]. Therefore, airfoils need to be optimized to be less sensitive to roughness.

Using a direct method based on a shape perturbation function [5], we designed two new airfoils with thickness to chord ratios of 30 and 36%. The objective was to create thick airfoils with good aerodynamic features and low roughness sensitivity. The optimization algorithm was coupled with a viscous/inviscid flow solver XFOIL.

A wind tunnel experiment was performed in the LM Wind Power low speed wind tunnel. The results from the experiment for DTU-230 and DTU-236 are discussed in the chapter.

77.2 Airfoil Design

Inverse design methods have been used in airfoil design since 1980 [6]. They are used when a desired airfoil surface pressure distribution at a given operating condition is prescribed, which is then translated into the corresponding geometrical shape. Since the surface flow is taken only at a single design point, this method has limitations regarding multiple design points.

Alternatively, direct design methods are more flexible and allow multidisciplinary optimization with multiple constraints. A numerical optimization algorithm can be coupled with a general flow solver where the response parameters can be directly used as design objectives. In this study, a commercial gradient-based constrained optimization algorithm [7] was coupled with the XFOIL code [8].

77.2.1 Design Method

The new airfoil shapes were created by modifying an existing airfoil using a shape perturbation function. This method is based on adding smooth perturbations to an initial airfoil. The smooth perturbations Δy are a linear combination of base functions P_k as

$$\Delta y(i) = \sum_{k=1}^{N} \delta_k P_k(i)$$

Base functions can be chosen to be any set of smooth functions [9]. This study is based on the work of [5]. The airfoil is split to an upper and a lower side with leading edge and trailing edge points fixed at $x=0$ and $x=1$, and the corresponding perturbation functions can be written for the upper surface as

$$\Delta y_u(i) = \sum_{k=1}^{N} \delta_{ku} P_{ku}(i)$$

and for the lower surface as

$$\Delta y_l(i) = \sum_{k=1}^{N} \delta_{kl} P_{kl}(i)$$

The shape functions for the upper and lower surface along the x-coordinate are

$$P_{ku}(i) = \sin^{\xi}(\pi x_u(k,i)^{g(k)})$$

and

$$P_{kl}(i) = \sin^{\eta}\left(\pi x_l(k,i)^{g(k)}\right)$$

The subscripts u and l symbolize the upper and lower surface of the airfoil, k is the index of the shape modes and i is the index of x and y coordinates. Variable g corresponds to the location of maximum of the base function. This variable is defined by the designer and gives him more influence on the decision-making process.

77.2.2 Optimization

The optimization objective was to maximize lift coefficient and lift-to-drag ratio. The objective function was expressed as

$$obj = \min\left(\frac{1}{C_p}\right), C_p = f(C_L, \frac{L}{D})$$

The coefficients C_L and L/D were weighted for clean and rough conditions with more emphasis on the rough case.

The objective function was identified as a smooth non-linear constrained function so "fmincon" from the MATLAB optimization toolbox was chosen as the appropriate solver. The solver algorithm was set to "SQP".

As previously mentioned, the optimization algorithm was coupled with a flow solver XFOIL [8]. The Reynolds number was set to 3×10^6 and the accounted angles of attack varied between 0° and 10°. This set of angles of attack was chosen to keep the lift coefficient in the linear region, which made the calculations more reliable. Free transition was modelled e^N with the envelope method with $N=9$ as the default value. Transition was forced by fixing the upper and the lower transition points at 5%, and 10% chords from the leading edge.

In this study, the initial airfoil for the design method was DTU-LN221. This is an airfoil previously developed at DTU and was chosen as a good starting point.

The DTU-LN221 has a favourable after stall behaviour, and assures that the created airfoil will belong to the new airfoil family.

Response parameters from XFOIL were used either directly as design objectives (lift coefficient and lift/drag ratio) or they were bounded in a constraint function (boundary layer thickness or lift coefficient degradation in the forced case). Other constraints imposed came from structural requirements such as position of maximum thickness, skewness of the airfoil, trailing edge thickness, etc.

The weighting coefficients or amplitudes δ_{ku} and δ_{kl} from the shape functions were the design variables, and with the two additional power factors of ξ,η the total number of design points was $2N+2$[5].

The objective of this study was to create high performing, low noise wind turbine airfoils that can accommodate a more demanding internal structure. Structural integrity was indirectly expressed through a concept of effective thickness to chord ratio. This is defined by the value of moment of inertia of a spar cap on the actual blade compared to the one which is uniform over the same width at the maximum relative thickness [10].

77.2.3 Optimization Results

The resulting DTU-230 and DTU-236 airfoils are shown in Fig. 77.1 together with three other airfoils in the same new family of airfoils DTU-LN2xx. It can be noted that the new thick airfoils have a very good shape compatibility with the middle thickness airfoils.

In order to see the performance of the DTU-230 airfoil, comparisons with two commonly used wind turbine airfoils—NACA 63-430 and FFA-W3-301 are carried out. Figure 77.2 shows the lift coefficients and lift-to-drag ratio of the three airfoils versus angle of attack for both clean and rough case. The coefficients have been computed with XFOIL for an angle of attack range of 0°–20° with a step 0.5°, $Re=1.47\times10^6$, $N=9$. Rough surface cases were simulated with a fixed transition of

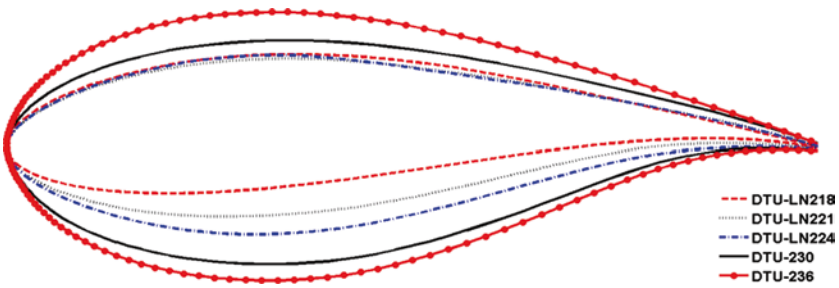

Fig. 77.1 New airfoil family DTU-LN2xx

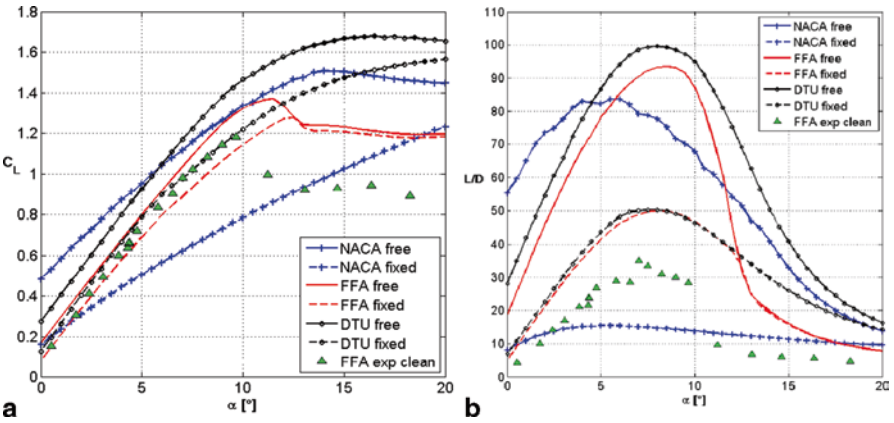

Fig. 77.2 Comparison of performance of airfoils NACA 63-430, FFA-W3-301 and DTU-230. *Left*: lift coefficients versus angle of attack; *Right*: lift to drag ratio versus angle of attack. The coefficients were computed with XFOIL for angle of attack range 0–20° with a step 0.5°, $Re = 1.47 \times 10^6$ with free and fixed transition (*5% suction, 10% pressure side*). The experimental data are for airfoil FFA-W3-301, clean surface, $Re = 1.47 \times 10^6$

5% chord on the suction side and 10% on the pressure side. Results are compared with experimental data for FFA-W3-301 measured in clean case at $Re = 1.47 \times 10^6$[3].

As can be noted, DTU-230 has higher maximum lift coefficient in both rough and clean cases. The difference between the maximum lift coefficients in the rough and the clean case, that is, roughness sensitivity is also quite good for DTU-230. The least roughness sensitive airfoil is FFA-W3-301; however, this merit was paid by a rather low lift. Comparison of lift-to-drag ratio over a set of angles of attack demonstrates that DTU-230 is the highest performing airfoil (Fig. 77.2, right).

77.3 The Experiment

77.3.1 The Wind Tunnel

The wind tunnel at LM Wind Power is a closed circuit, variable fan speed tunnel, with a cooling system to ensure constant flow temperature. The flow quality is very high with turbulence intensity levels around 0.1%. The tunnel has a contraction of 10–1 and is equipped with specially designed corner vanes, a honeycomb structure and three fine mesh screens. The width of the test section is 1.35 m and the height is 2.7 m. The model chord length of 0.9 m at the maximum wind speed of 105 m/s gives a chord Reynolds number of 6×10^6 and a Mach number of $M = 0.3$.

77.3.2 The Measurement Campaigns

The DTU-230 and DTU-236 airfoils were tested at several Reynolds numbers and in different surface configurations with different devices (such as vortex generators and Gurney flaps). The tested Reynolds numbers were $Re = 1.5$, 3, 4, 5 and 6×10^6. The airfoil performance in rough conditions was investigated using a standard zig-zag tape and bump tape. Data presented in this chapter are the measurements with zigzag tape of 0.4 mm thickness placed at 5% chord on the suction side and 10% chord on the pressure side.

77.4 Results and Discussions

77.4.1 DTU-230

Figure 77.3 shows a comparison of expected lift coefficients calculated with XFOIL and measured ones. The most noticeable result is that XFOIL over predicts lift and does not capture stall effects. The XFOIL was developed primarily for thin airfoils so this behaviour was expected. In the linear region, the difference is not that big but as soon as stall approaches, the difference between the calculated and measured data is greater. Therefore, the decision to limit the angle of attack to 10° in the optimization proves to be valid. The same effect can be observed when the zigzag tape is applied to the test model surface; only in this case, the difference is more pronounced already at lower angles of attack. The airfoil with "tripped" boundary

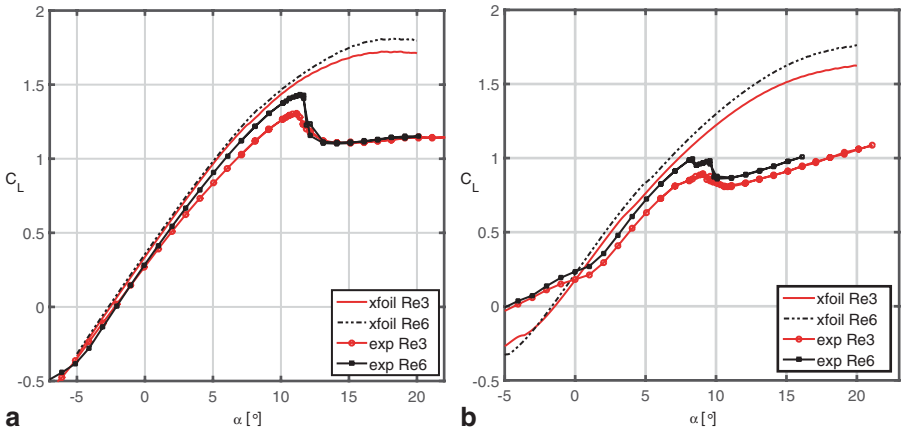

Fig. 77.3 DTU-230–Comparison of lift coefficients versus angles of attack computed with XFOIL and experimental data from LM wind tunnel at Reynolds numbers = 3 and 6 million. *Left*: free transition in XFOIL and clean surface of the test model; *Right*: forced transition in XFOIL and applied zigzag tape at 5% chord on the suction side and 10% chord on the pressure side of the test model

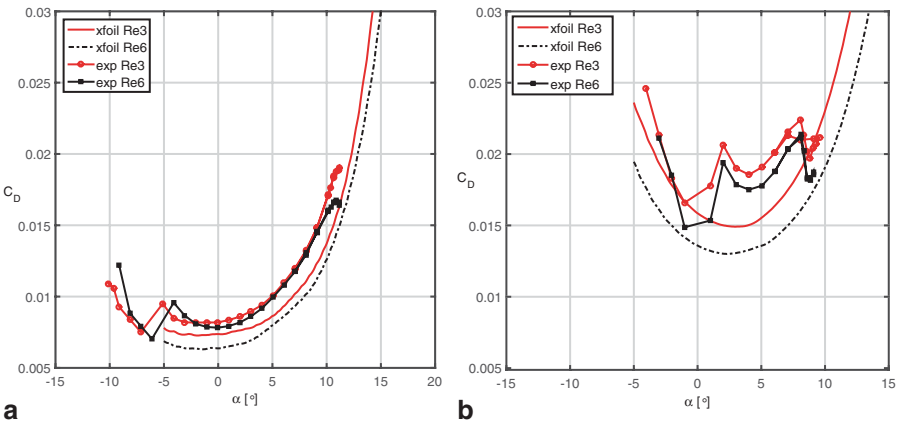

Fig. 77.4 DTU-230–Comparison of drag coefficients versus angles of attack computed with XFOIL and experimental data from LM Wind tunnel at Reynolds numbers = 3 and 6 million. *Left*: free transition in XFOIL and clean surface of the test model; *Right*: forced transition in XFOIL and applied zigzag tape at 5% chord on the suction side and 10% chord on the pressure side of the test model

layer stalls at around 8° so the range of angles of attack in optimization could have been even more conservative. The power coefficient in the objective function was a blended function of both the clean and the rough cases. Since the ranges of attack should be different for those cases, the power coefficient should have been also adjusted to that.

The obvious change of zero lift angles between "clean" and "tripped" airfoils was expected and is similar to that in cases with other thick airfoils [3].

When looking into drag coefficients (Fig. 77.4) the opposite can be observed: XFOIL is under predicting. Although drag coefficients were obtained from pressure taps on the airfoils, load cells and a wake rake, only the data from the wake rake are shown here. To protect the wake rake in stall conditions, it was removed from the wake just before the stall point.

The effect of increasing Reynolds number can be seen in both lift and drag coefficients—the lift increases and the drag decreases.

The overall properties of the DTU-230 are quite good. The aerodynamic characteristics are satisfactory and its geometrical simplicity and compatibility with the whole DTU-2xx family is an advantage for manufacturability and reliability. This ensures that the performance of the blade built with this airfoil will match the designed performance.

77.4.2 DTU-236

The DTU-236 airfoil was quite challenging to measure due to the large relative thickness and a high aspect ratio of the test model (aspect ratio = 1.5). To alleviate the problem of returning flow stall cells forming on the side edges of the airfoil, the

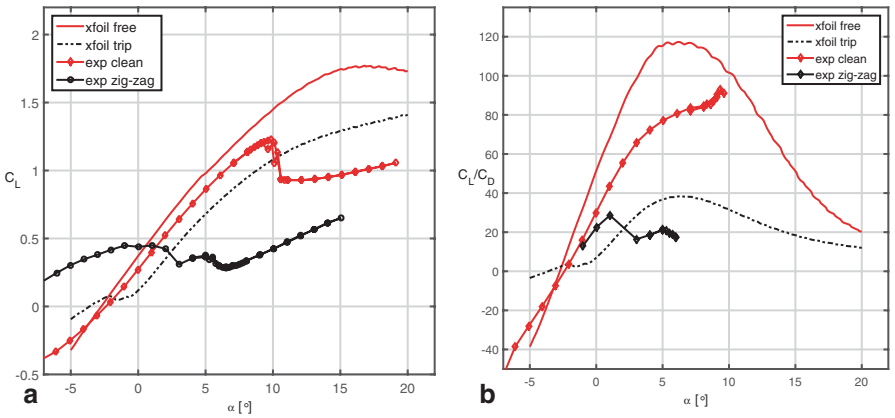

Fig. 77.5 DTU-236–Comparison of lift coefficients and lift-to-drag ratio versus angles of attack computed with XFOIL and experimental data from LM Wind tunnel at Reynolds number = 6 million; test model surface condition—clean and with applied zigzag tape at 5 % chord on the suction side and 10 % chord on the pressure side, corresponding free and forced (*trip*) boundary layer transitions in XFOIL. Only drag coefficients measured with a wake rake are included in the lift-to-drag ratio plot

wall boundary layers were energized using a blowing system built in the sidewalls of the test section. The results shown in Fig. 77.5 are only for the highest measured Reynolds number (6 million). As was the case with the DTU-230, the angle of attack was limited to 10° in the optimization. Given that the airfoil is stalled around 9° in the clean case, this limit should have been set to a lower angle. Only wake rake drag measurements are included in the lift-to-drag ratio plots. Since the airfoil stalled at around 9° and 6° in clean and tripped surface conditions, the data range is rather small.

Figure 77.5 also shows an even greater discrepancy in calculated and measured lift coefficients than with the DTU-230. This clearly proves XFOIL was not designed to handle such thick airfoils and should be used with precaution. Results for "tripped" calculations and data obtained while a zigzag tape was applied to the model surface indicate neither of the results should be trusted: XFOIL because it was not made for such cases and the experimental data should be verified in a tunnel with less blockage or with a smaller model. One possibility for this particular wind tunnel would be to use a model with a shorter chord line, for example choosing a length of 0.6 m. A smaller absolute thickness and larger aspect ratio would reduce the tunnel blockage but the maximum achievable Reynolds number in that case would be around 4 million. That is a compromise worth investigating.

Numerical flow solvers should receive more attention since neither the existing panel codes nor the computational fluid dynamics (CFD) codes have the ability to accurately capture stall and post stall behaviour of very thick airfoils compared to wind tunnel tests, even though the CFD performs a bit better as is shown in [11].

Given the high relative thickness and a small camber, the DTU-236 airfoil performs quite well. Rotational effects were not included in this analysis, but are assumed to lessen the roughness sensitivity [2].

77.5 Conclusion

The introduced design method is an effective tool to develop thick high performing wind turbine airfoils. The shape perturbation function was integrated in a numerical constrained optimization algorithm coupled with XFOIL. The results from the wind tunnel confirmed that using XFOIL in the linear region for DTU-230 was reasonable. However, for the very thick airfoils, using a CFD may have been a better option and should be considered in the future even though it is much more time-consuming.

Since the optimization process is rather fast, the design could be further improved with constraints that are more elaborate without significantly influencing the optimization performance.

References

1. Vestas Wind Systems A/S (2014) World's most powerful wind turbine now operational. http://www.vestas.com/en/media/news#!140128_nr_vws. Accessed 31 July 2014.
2. Timmer W, van Rooij R (2003) Summary of the delft university wind turbine dedicated airfoils. J Solar Energy Engg 125(4):488–496
3. Bertagnolio F, Sorensen N, Niels N, Johansen N, Fuglsang P (2001) Wind turbine airfoil catalogue. Tech.rep., Risø-R-1280(EN).
4. Sareen A, Chinmay SA, Selig MS (2013) Effects of leading edge erosion on wind turbine blade performance. Wind Energy. doi:10.1002/we.1649
5. Zhu WJ, Shen WZ (2013) Integrated airfoil and blade design method for large wind turbines, Proceeedings of the 2013 International Conference on Aerodynamics of Offshore Energy Systems and Wakes, Lyngby, Denmark, pp. 318–326
6. Eppler R, Somers DM (1980) A computer program for the design and analysis of low speed airfoils, NASA TM.80210.NASA Langley Research Center, Hampton
7. MATLAB (2012) version 8.00.783 (R2012b). The Math-Works Inc., Natick
8. Drela M (1989) Xfoil: an analysis and design system for low reynolds number airfoils. In: Mueller T (ed) Low reynolds number aerodynamics, vol 54 of lecture notes in engineering. Springer Berlin, Heidelberg, pp. 1–12.
9. Hager J, Eyi S, Lee K (1994) Two-point transonic airfoil design using optimization for improved off-design performance. J Aircraft 31(5):1143–1147
10. Jamieson P (2011) Innovation in wind turbine design, 1st edn. Wiley, West Sussex
11. Zahle F, Bak C, Sørensen N et al (2014) Design of the LRP airfoil series using 2D CFD. J Phys: Conference Series 524